

Terrestrial remote sensing science and algorithms planned for EOS/MODIS

S. W. RUNNING

School of Forestry, University of Montana, Missoula, MT 59812, U.S.A.

C. O. JUSTICE

Department of Geography, University of Maryland, College Park, MD 20742, U.S.A.

V. SALOMONSON, D. HALL, J. BARKER, Y. J. KAUFMANN

NASA/Goddard Space Flight Center, Greenbelt, MD 20771, U.S.A.

A. H. STRAHLER

Center for Remote Sensing, Boston University, Boston, MA 02215, U.S.A.

A. R. HUETE

Department of Soil and Water Science, University of Arizona, Tucson, AZ 85721, U.S.A.

J.-P. MULLER

Department of Photogrammetry and Surveying,
University College of London WC1E 6BT, England, U.K.

V. VANDERBILT

NASA Ames Research Center, Moffett Field, CA 94035, U.S.A.

Z. M. WAN

Computer System Lab./CRSEO, University of California at Santa Barbara,
Santa Barbara, CA 93106, U.S.A.

P. TEILLET

Canada Centre for Remote Sensing, 588 Booth St., Ottawa, Ontario,
Canada K1A 0Y7

and D. CARNEGIE

U.S.D.I. Geological Survey, EROS Data Center, Sioux Falls, SD 57198,
U.S.A.

Abstract. The Moderate Resolution Imaging Spectroradiometer (MODIS) will be the primary daily global monitoring sensor on the NASA Earth Observing System (EOS) satellites, scheduled for launch on the EOS-AM platform in June 1998 and the EOS-PM platform in December 2000. MODIS is a 36 channel radiometer covering 0.415-14.235 μm wavelengths, with spatial resolution from 250 m to 1 km at nadir. MODIS will be the primary EOS sensor for providing data on terrestrial biospheric dynamics and process activity. This paper presents the suite of global land products currently planned for EOSDIS implementation,

to be developed by the authors of this paper, the MODIS land team (MODLAND). These include spectral albedo, land cover, spectral vegetation indices, snow and ice cover, surface temperature and fire, and a number of biophysical variables that will allow computation of global carbon cycles, hydrologic balances and biogeochemistry of critical greenhouse gases. Additionally, the regular global coverage of these variables will allow accurate surface change detection, a fundamental determinant of global change.

1. Introduction

1.1. Global science issues

As quoted from the United States Global Change Research Program (USGCRP) report, 'The central goal of the USGCRP is to establish the scientific basis in support of national and international policy-making relating to natural and human-induced changes in the global Earth system, by: "Establishing an integrated, comprehensive long-term program of documenting the Earth system on a global scale; Conducting a program of focusing studies to improve our understanding of the physical, geological chemical, biological and social processes that influence Earth system processes; Developing integrated conceptual and predictive Earth systems models"' (CEES 1992). In that same USGCRP report, the role for NASA of the Earth Observing System (EOS) is to '...provide an integrated, comprehensive monitoring and data management program of simultaneous measurements of key global change variables'.

In the report to Congress from NASA on Restructuring of the Earth Observing System, dated 9 March 1992, seven key science objectives are stated, and have been reiterated by both Intergovernmental Panel on Climate Change (IPCC 1991) and USGCRP reports (Asrar and Dokken 1993). Two of these objectives are central to the role of the MODIS land science team, MODLAND in EOS, '... the sources and sinks of greenhouse gases, and their atmospheric transformations', and '... changes in land use, land cover, primary productivity and the water cycle,' (Asrar and Dokken 1993).

These science objectives illustrate there are fundamental questions of global change that are still unanswered. The analysis by Tans *et al.* (1990) shows that scientists still cannot decide whether the terrestrial biosphere is a source or sink of CO₂. More fundamentally, Townshend *et al.* (1991) show that scientists cannot even agree on the areal extent of basic global land cover classes. Clearly, understanding and monitoring the carbon balance and hydrologic balance of the terrestrial biosphere is fundamental to these two science objectives of U.S. global change research, EOS, and the international research community (IGBP 1990).

On technical issues, Goward *et al.* (1991) state that errors of ± 50 per cent are possible in the two channel Normalized Difference Vegetation Index (NDVI) currently used for global vegetation studies, when derived from the NOAA Global Vegetation Index product (James and Townshend 1994). These errors result from poor sensor calibration, poor image navigation, incomplete cloud screening, variable spatial resolution and inadequate on-board data storage. Improvements in atmospheric corrections to remove haze, aerosols and clouds from land surface images require higher spectral and radiometric resolution than AVHRR currently provides (King *et al.* 1992). As the demands of global science evolve from simple qualitative mapping to quantitative monitoring, these errors limit the use of NDVI from the AVHRR as a direct measure of biospheric processes.

In this context of global change research priorities, the Moderate Resolution Imaging Spectroradiometer (MODIS) of the EOS has the highest responsibility for producing regular full Earth terrestrial coverage (figure 1). MODIS will be the primary EOS sensor for providing data on terrestrial biospheric dynamics and process rates. A suite of MODIS land products is currently planned for EOSDIS at-launch (figure 2). These include spectral albedo, land cover, spectral vegetation indices, snow and ice cover, surface temperature and fire, and a number of biophysical variables that are necessary for computation of global carbon cycles, hydrologic balances and biogeochemistry of critical greenhouse gases. Additionally the regular global coverage of these variables will allow accurate change detection, the most fundamental determinant of global change.

1.2. History of EOS

Planning for the NASA Earth Observing System began in 1983, and in 1988 an Announcement of Opportunity was issued to the world science and engineering community to formally select science investigations of EOS and a science team for each sensor; these selections were made public in 1989 (Asrar and Dokken 1993).

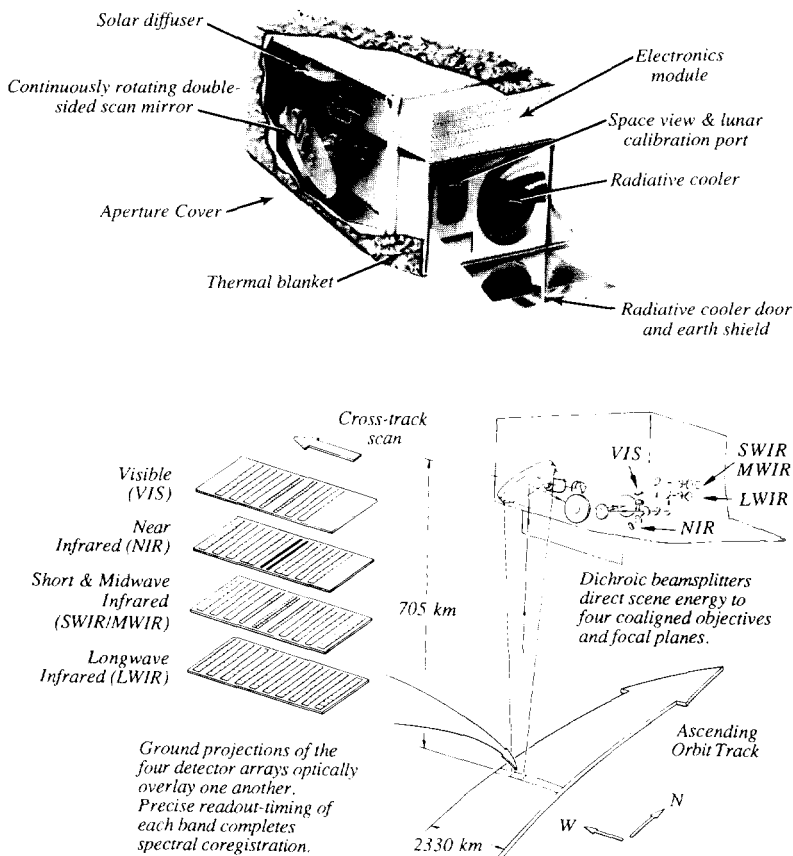


Figure 1. Diagrammatic sketch of the Moderate Resolution Imaging Spectroradiometer (MODIS) (provided by Santa Barbara Research Center).

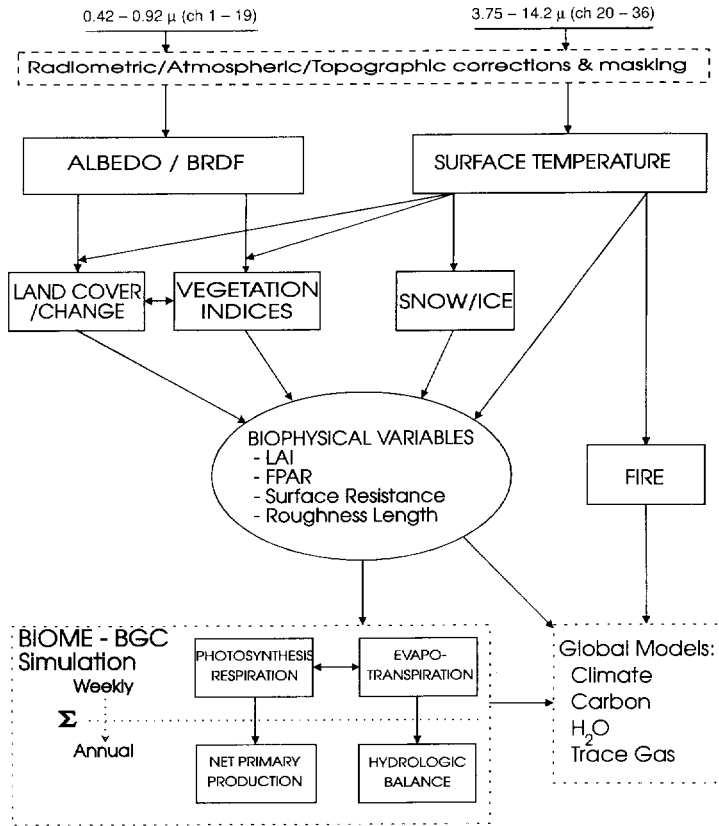


Figure 2. Logical flowchart of the products planned for development by the MODIS land science team (MODLAND) for implementation in EOS.

The authorization of a NASA new start for EOS, and Mission to Planet Earth was made by the U.S. Congress in October, 1990, and the first platform of sensors that included MODIS, called EOS-A was selected for a scheduled launch of 1998, with an EOS-B to follow in 2002. After the Congressionally mandated rescoping of EOS in 1992, the new configuration was chosen of a morning overpass EOS-AM platform to be launched in June 1998, followed by an afternoon EOS-PM platform to be launched in 2000. Both EOS-AM and EOS-PM are polar orbiting sun-synchronous platforms, that differ in their component of sensors and overpass timing, currently planned at ascending 10.30 and descending 13.30 hours equatorial crossing times respectively. Quoting from the NASA report to Congress about restructuring EOS, 'Moreover, MODIS is the central instrument on EOS, and with it flying on two separate spacecraft the program has important redundancy' (Asrar and Dokken 1993).

2. MODIS philosophy and objectives

The guiding philosophy of MODIS design is to produce a regular global dataset of well calibrated data of high radiometric resolution for a wide array of earth system sciences. MODIS will be a substantial improvement over the current

AVHRR sensor in spatial resolution (250 m, 500 m and 1 km versus 1.1 km, see figure 3), spectral coverage (36 channels versus 5 channels), with on-board calibration and comprehensive improvements in radiometric accuracy. These spectral bands and radiometric characteristics have been carefully selected to enable improved studies of land, ocean and atmospheric processes. Finally, the philosophy of EOS is to provide most regular processing with the EOS Data Information System (EOSDIS), removing high volume, repetitive tasks from the end-user community.

The land science members of the EOS MODIS team (MODLAND) have responsibility for developing the land surface remote sensing algorithms that will be produced in EOSDIS from the MODIS sensors. The objective of this paper is to describe the current status of remote sensing products planned by the MODLAND team for the use of EOS scientists in global ecological research; these will be made available through EOSDIS to the general science community for research projects world-wide. MODLAND responsibilities range from definition of data pre-processing procedures, to formulation of algorithms to provide 'standard' EOSDIS global land products, testing and evaluation of standard products, postlaunch research and development of new products, and global scale terrestrial science using the MODIS sensor.

3. MODIS sensor configuration

MODIS will provide data between 0.415–14.235 μm with spatial resolutions of 250 m (2 bands), 500 m (5 bands) and 1000 m (29 bands) (tables 1, 2). Development of the spectral requirements for these MODIS bands has included considerations such as the avoidance of Fraunhofer lines in the solar irradiance spectrum, avoidance of atmospheric absorption lines and inclusion of key features in target spectra.

MODIS is designed to scan through nadir in a plane perpendicular to the velocity vector of the spacecraft (figure 1). The maximum scan extends 55° on either side of nadir (110° aperture), yielding a swath width of 2330 km centred on the satellite ground track. The orbital altitude planned is 705 km on a 16 day, 233 orbit repeat cycle for the EOS-A platform (Asrar and Dokken 1993). The orbital average data rate of MODIS will be 5.1 Mbps (55 Gbyte per day).

The emitted and reflected solar radiation from the Earth are incident on a scan mirror canter 45° to the long axis of the instrument, followed by a telescope and a sequence of two dichroic beam splitters that further subdivide the incoming radiation into four focal planes. Each spectral band uses a ten element linear array detector for the 100 m spatial resolution bands (channels 8–36), a 20 element array for the 500 m bands (channels 3–7) and a 40 element array for the 250 m bands (channels 1–2). Each array is aligned parallel to one another such that a single scan of the scan mirror is imaged on the focal plane for a swath 10 km in the along track direction. In this configuration all channels within each focal plane are simultaneously sampled and coregistered, with registration errors of less than 100 m between focal planes. However, currently the pixel locational registration is stated to be only 200 m between focal planes, a specification of great concern for change detection studies of land cover.

A critical requirement for the land community is that the pixels from each band be inherently registered to at least 0.2 pixel, with a stated goal of 0.1 pixel, or 100 m for the 1 km pixels. Thus data from the different bands and different orbital passes

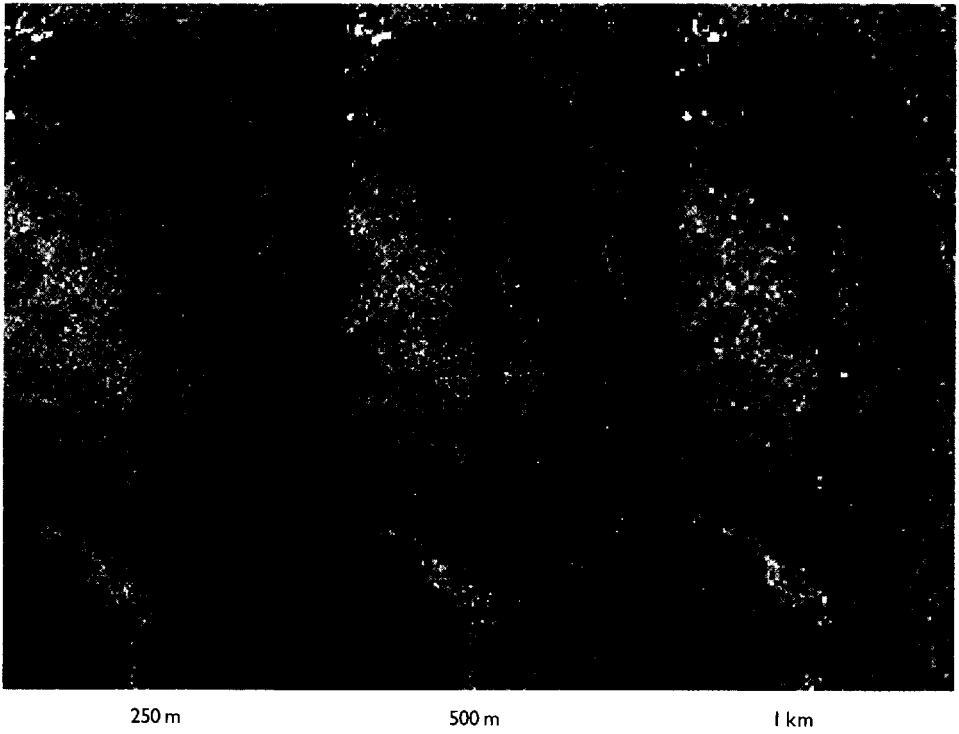


Figure 3.

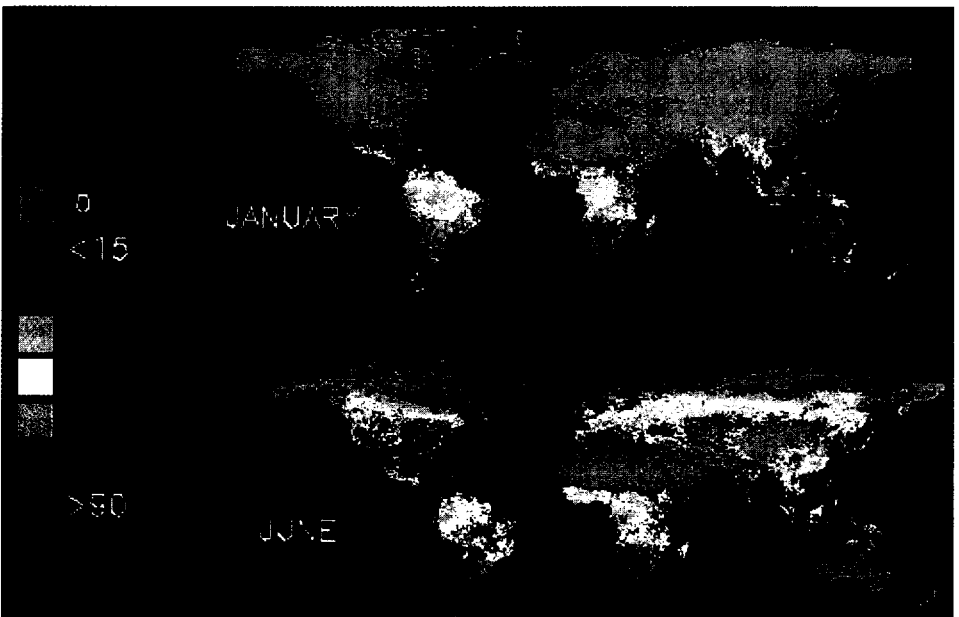


Figure 12.

Table 1. MODIS instrument requirements.

Variable/parameter	Symbol	Requirement
Equatorial crossing time	t	10.30 AM descending EOS-AM orbit platforms 1.30 PM ascending EOS-PM orbit platforms
Platform altitude	H	705 km
Number of spectral bands	N	36 from 0.41 to 14.4 μm
Ground swath	GFOV	2330 km along-scan by 10–20 km along-track
Angular swath	FOA	$\pm 55^\circ$ along-scan by 14 milliradians along-track
Ground resolution	GIFOV	Band-dependent 250 m, 500 m and 1000 m @ nadir Band-dependent 375 m, 750 m and 1500 m at $\pm 45^\circ$ Band-dependent 500 m, 1000 m and 2000 m at $\pm 55^\circ$
Angular resolution	IFOV	0.354 mr, 0.709 mr, 1.418 mr (all $\pm 6\%$)
Band-to-band registration	BBR	< 0.1 IFOV goal, < 0.2 IFOV requirement (3σ)
Quantization	n	10–12 Bit (to meet Signal-to-Noise (SNR) Spec)
Modulation transfer function	MTF	0.3 at Nyquist frequency
Polarization factor insensitivity	PF	$< 2\%$, 0.41 to 2.2 μm
Volume (length \times width \times height)	V = l \times w \times h	$< 1 \times 1.6 \times 1$ m
Mass	M	< 250 kg
Power	P	< 225 W average, < 275 W peak
Operating/duty cycle	OC	100%
Data rates (with overhead)	DR	< 11 Mbps (day mode) < 3 Mbps (night mode)
Pointability angle of optical axis	PA	$\pm 20^\circ$ from horizon (full phase of moon)
Absolute radiometric accuracy	AL	$\pm 5\%$ (1σ) $\leq 3 \mu\text{m}$, $\pm 1\%$ (1σ) $> 3 \mu\text{m}$
On-orbit reflectance precision	PR	$\pm 2\%$ (1σ) $\leq 3 \mu\text{m}$ relative to the Sun

can be compared directly on the ground, and multi-band geophysical information can be produced without the loss of resolution caused by spatial resampling to correct misregistration. This geographical registration requirement, essential for time series and land surface change detection analyses, is currently one of the most challenging engineering specifications for MODIS.

4. Data preprocessing and calibration

4.1. In-flight calibration and registration

The experience of Earth Scientists assembling multi-year data sets of satellite imagery for change detection, e.g., using AVHRR imagery to produce NDVI maps, has led to the placing of a strong requirement on the MODIS instruments to be well calibrated and characterized over their entire operational lifetimes. The imagery collected from all six planned MODIS instruments in the EOS/Mission to Planet Earth must be capable of being merged into a single 15-year data set.

Figure 3. A comparison of the spatial resolutions to be produced by MODIS at 1 km (current AVHRR resolution), 500 m and 250 m pixel sizes. The scene shown, from western Montana, USA, exhibits high variability in topography and land covers; including bare rock, snow/ice, water, evergreen needleleaf forest, deciduous needleleaf forest, deciduous broadleaf shrubland, grassland, cropland and urban. Produced from the subsampled Landsat-TM image of 20 July 1991. (Provided by J. White). RGB colour bands 4, 5, and 3. Area = 168 by 67 km.

Figure 12. A sample of the dynamic, biome specific net photosynthesis product planned for implementation globally using the procedures from figure 11. This global computation is based on AVHRR/NDVI and surface climate for 1990. (Provided by R. Nemani).

Table 2. Channel specifications for the MODIS sensor.
(a)

Band N	Ground resolution GIFOV (m)	FWHM band pass*		Primary scientific purpose
		Lower bandpass λ Min (nm)	Upper bandpass λ Max (nm)	
1	250	620	670	Vegetation chlorophyll absorption Land cover transformations Cloud/edge detection/masks
2	250	841	876	Cloud/vegetation/water/edge detection Land-cover transformations/masks
3	500	459	479	Soil and vegetation differences
4	500	545	565	Green vegetation
5	500	1230	1250	Leaf and canopy properties
6	500	1628	1652	Snow and cloud differences/masks
7	500	2105	2155	Land and cloud properties
8	1000	405	420	Water colour (chlorophyll/pigments/sediments) Atmospheric scattering/cloud mask
9	1000	438	448	Water colour
10	1000	483	493	Water colour
11	1000	526	536	Water colour
12	1000	546	556	Sediments
13	1000	662	672	Sediments, atmosphere
14	1000	673	683	Chlorophyll fluorescence
15	1000	743	753	Aerosol properties
16	1000	862	877	Aerosol and atmospheric properties
17	1000	890	920	Water vapour/atmospheric properties
18	1000	931	941	Water vapour/atmospheric properties
19	1000	915	965	Water vapour/atmospheric properties
26	1000	1360	1390	Cirrus cloud/cloud mask

*FWHM (Full Width at Half Maximum) = λ Max - λ Min, where λ Max = $\lambda_c + (BW/2)$ and λ Min = $\lambda_c - (BW/2)$.

Ref: NASA, 1992, NASA/GSFC/EOS Document: MODIS-N Spec., as amended to 29 December 1992, Ref # 422-20-02, Greenbelt, MD 20771, U.S.A.
Continues

Both spectral and radiometric in-flight calibrations are planned for the MODIS sensors. Spectral calibration involves determining the wavelength range falling on each detector as a function of instrument temperature and lifetime. The calibration will be done on-board with an accuracy to detect shifts of ± 1 nm for wavelengths shorter than $1 \mu\text{m}$. The on-board calibrators and sensor-based methods consist of the Spectro-Radiometric Calibration Assembly, (SRCA), the Solar Diffuser (SD) Plate and associated Solar Diffuser Stability Monitor (SDSM), Blackbody (BB), and a view of space and the Moon (figure 1).

SRCA: The SRCA is a $1/4$ aperture calibration instrument on MODIS that provides an active on-orbit method that can characterize spectral ($0.4 \leq \lambda \leq 2.0 \mu\text{m}$) and spatial (all bands) changes in the instrument performance characteristics, in addition to providing both a pre-launch to on-orbit traceable

Table 2. (b)

Band N	Ground resolution GIFOV (m)	FWHM band pass*		Primary scientific purpose
		Lower bandpass λ_{Min} (nm)	Upper bandpass λ_{Max} (nm)	
20	1000	3660	3840	Sea surface temperature
21	1000	3931	3987	Forest fires/volcanoes
22	1000	3929	3989	Cloud
23	1000	4020	4080	Cloud/surface temperature/cloud mask
24	1000	4433	4498	Cloud/surface temperature/cloud mask
25	1000	4482	4549	Tropical temperature/cloud fraction
26	Moved to Table 2(a)			
27	1000	6535	6895	Tropical temperature/cloud fraction
28	1000	7175	7475	Mid-tropical humidity
29	1000	8400	8700	Upper-tropical humidity
30	1000	8980	9880	Surface temperature/cloud mask
31	1000	10780	11280	Total ozone
32	1000	11770	12270	Cloud/surface temperature
33	1000	13185	13485	Cloud/surface temperature
34	1000	13485	13785	Cloud height and fraction
35	1000	13785	14085	Cloud height and fraction
36	1000	14085	14385	Cloud height and fraction

*FWHM (Full Width at Half Maximum) = $\lambda_{\text{Max}} - \lambda_{\text{Min}}$, where $\lambda_{\text{Max}} = \lambda_c + (\text{BW}/2)$ and $\lambda_{\text{Min}} = \lambda_c - (\text{BW}/2)$.

Ref: NASA, 1992, NASA/GSFC/EOS Document: MODIS-N Spec., as amended to 23 December 1992, Ref # 422-20-02, Greenbelt, MD 20771, U.S.A.

absolute radiometric transfer standard for the solar diffuser ($0.4 \leq \lambda \leq 2.2 \mu\text{m}$) and a within-orbit radiometric calibration mechanisms.

SD/SDSM: The solar diffuser is designed to provide two ranges of radiances that differ by a factor of ten to cover the dynamic range of all the reflective bands whenever the SD door is open when passing over the North Pole. The SDSM is designed to alternately look at the Sun and the SDE, providing radiometric calibration of 2 per cent precision.

BB: The full-aperture blackbody is an aluminium plate with V-grooves cut at 25° half angles, painted with a specular black paint to provide a high effective emissivity (≥ 0.992). The blackbody will be allowed to float thermally and its temperature monitored to an accuracy of 0.1 K.

Space view: Space is viewed once per scan by all the bands through the space port. For the emissive bands, this will provide the second temperature calibration point for a linear calibration.

Lunar: A lunar radiometric calibration of the reflective bands on a timescale of 2–5 years is provided by the Moon passing through the view of the space port two to six times per year at approximately 22.5° beyond the first lunar quarter.

4.2. Atmospheric corrections

A variety of atmospheric properties important to land remote sensing are planned to be produced from MODIS data, including cloud characteristics, aerosols

and water vapour. Investigation of aerosol properties and their interaction with radiation will be critical in understanding remotely sensed data, and for designing and validating remote sensing aerosol retrieval (Kaufman and Sendra, 1988, Tanré *et al.* 1992) and atmospheric correction systems (Holben *et al.* 1991, 1992). King *et al.* (1992) provide a comprehensive presentation of the theory and algorithms planned, which will only be summarized here.

Fractional cloud cover is important for land remote sensing as a mask to exclude cloud contaminated pixels, and for cloud shadows. Of greater difficulty is the discrimination between snow or ice-covered land and clouds. MODIS cloud identification will use a combination of shortwave and longwave reflectance thresholding, cloud top temperatures and spatial coherence for cloud definition. Atmospheric scientists are interested in cloud optical thickness, and the effective droplet particle radius for defining cloud type and solar energy balances. Aerosol optical thickness can be determined from certain highly absorbing spectral bands and over surfaces chosen to have low spectral reflectance. Various reflectance ratios of certain selected wavelengths are used for these computations of aerosol optical thickness (King *et al.* 1992). Precipitable water vapour is currently retrieved as a by-product of remotely sensed atmospheric temperature profiles. All of these atmospheric parameters are required to separate atmospheric from land-based spectral reflectance components of the received signals.

4.3. Topographic corrections

Crucial to the MODLAND research, particularly the land cover and MODIS Vegetation Index algorithms, will be the accurate removal of topographic effects which confuse the signal and lead to errors when trying to use multi-temporal sequences. Topography affects both the geometric and radiometric characteristics of MODIS data as well as being a key dataset for the development of numerical models for Earth Systems Science. Substantial topographic variability effects approximately 30 per cent of the Earth's surface, and will cause pixel shifts of greater than one pixel for 1 km bands, rising to over 60 per cent for the 250 m bands if these topographic features are not corrected for (Muller and Eales 1990, figure 4).

Topography will affect the accuracy of the retrieval of 'at surface reflectance' in three ways. The first level of topographic correction will take into account gross changes in terrain elevation as an atmospheric pathlength correction, to adjust for changes in scattering and absorptance transmittances of the atmosphere (Teillet and Staenz 1993). More accurate pixel-specific topographic correction for localized radiometric effects (slope/aspect related illumination differences, reflection from adjacent terrain, shadowing) will require highly accurate and well registered digital elevation data. Finally, it is hypothesized that sub-pixel shadowing will cause BRDF-like effects on the resultant images.

A global DEM (Digital Elevation Model) with 3 arc-second spacing, an elevation accuracy of at least 30 m and a slope accuracy of $1-3^\circ$ is needed for 250 m and 500 m MODIS pixels. For 1 km pixels, a global DEM with grid-spacing of 500 m (15 arc-seconds), an elevation accuracy of 100 m and a slope accuracy of 5° is required (Muller and Eales 1990). A global database for topographic corrections should be a key prelaunch activity by EOSDIS.

4.4. Binary masking

Binary masking is an important and computationally efficient initial processing step for categorizing raw radiance data into one of several broad surface categories

for subsequent detailed processing. Initially, the masking product will be three 32-bit images, one for each of the different 250, 500 and 1000 m MODIS spatial resolutions. The bits in these images are each masks containing binary (yes/no) information on each pixel on the definite presence or absence of: clouds, snow/ice, water, land, glint, vegetation, shadow, spectral outlier, spatial centre/edge, and day/night terminator lines. There will be different discipline-dependent masks for some of these classes and different algorithms will be developed for daytime and nighttime imagery.

5. MODLAND remote sensing products

The MODIS land products currently planned for EOSDIS at-launch are spectral albedo, land cover and land cover change, MODIS spectral vegetation indices, snow and ice cover, surface temperature and fire, and biophysical variables for advanced terrestrial ecosystem carbon and hydrologic budget algorithms, many requested by EOS Interdisciplinary Studies projects. MODLAND also will integrate these variables to execute simple global carbon and water budget models (figure 2).

5.1. Albedo and BRDF

Two types of albedo products are planned for MODIS. First reflectances from Channels 1-4 will provide a simple nadir broad-band surface albedo for global climate modelling that requires this key surface variable for shortwave energy partitioning. Second, multi-angle spectral albedos will be developed as a precursor to other advanced MODLAND products.

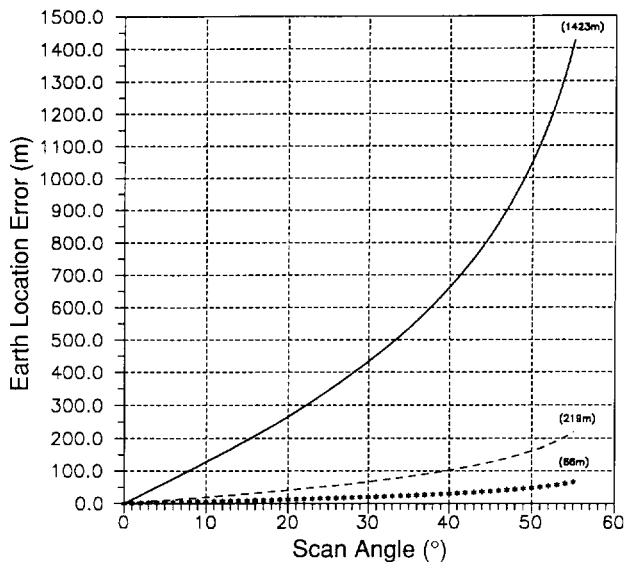


Figure 4. The potential for earth location error of a pixel caused by three sample terrain height errors, 30 m, 100 m or 650 m, at different sensor scan angles. This illustrates the necessity of a global topographic dataset to provide topographic corrections to MODIS data. (Provided by P. Hubanks). ***, 30 m terrain height error. ----, 100 m terrain height error. ———, 650 m terrain height error.

MODIS images at large view angles (maximum 55°) in the cross-track direction, giving the ability to make directional radiance measurements of the Earth's surface. MODIS will be complemented by the EOS MISR (Multi-angle Imaging Spectroradiometer, Diner *et al.* 1991, Asrar and Dokken 1993) a sensor with nine cameras at nine fixed viewing angles in the along track direction. Together these sensors will reveal many new characteristics of the three-dimensional structure of the land surface. Many land surface covers have highly anisotropic angular bidirectional reflectance distribution functions (BRDFs, see figure 5), and a large measure of the anisotropy is due to shadow patterns governed by the three-dimensional nature of the surface (Li and Strahler 1992).

Structural and radiometric data will be used to calibrate a number of appropriate canopy reflectance models, which will then be tested for their ability to reproduce BRDFs. These will be selected from a range of types, including geometric-optical (e.g., Li and Strahler 1992), plane-parallel radiative transfer (e.g., Verstraete *et al.* 1990), hybrid geometric radiative-transfer (e.g., Nilson and Peterson 1991), pure radiative-transfer (e.g., Myneni *et al.* 1990) and Monte Carlo (e.g., Kimes *et al.* 1985). We will simulate MODIS and MISR imagery, involving calculation of at-satellite radiances from the database at nine look angles—four forward and four aft, and one at nadir—at resolutions appropriate to the viewing geometry of each MISR camera (nominally 250 m at the centre of the scan). For MODIS, a suite of images must be simulated, each providing an image from a single overpass at one viewing geometry and Sun position. These simulations will include atmospheric effects as well as Sun-angle effects.

Given these simulated images, we will explore a number of possible algorithms for BRDF extraction. These will include not only statistical models that simply fit

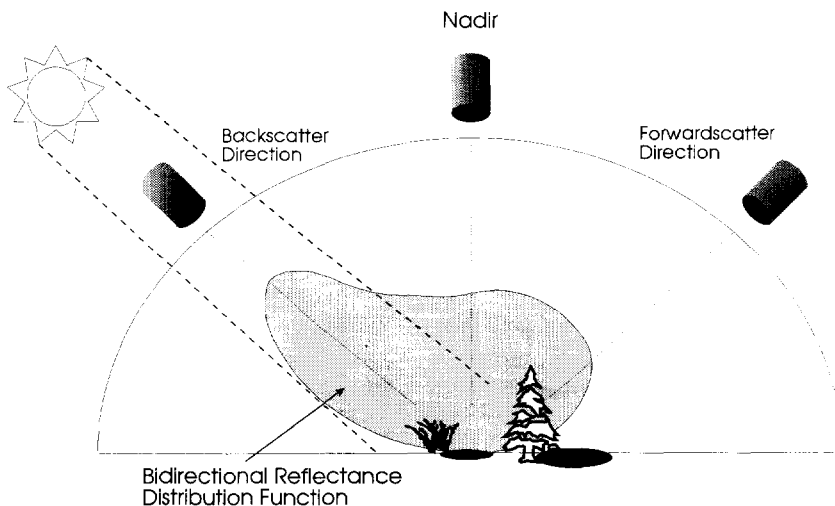


Figure 5. A conceptual diagram illustrating how directional remote sensing is used to evaluate the bi-directional reflectance distribution function (BRDF) and discriminate vegetation classes (redrawn from Irons *et al.* 1991).

the BRDF to the radiances observed, but also a selection of physically-based models, using geometric-optical and/or radiative-transfer theory, that can provide surface parameter inference through inversion in practical circumstances. These BRDF products will then be used in development of MODLAND products, particularly the land cover and MODIS spectral vegetation indices, and biophysical variables such as roughness length and leaf area index.

5.2. Land cover and land cover change

The MODLAND Group is responsible for the development of two products that will be of wide use in EOS, a land cover product that will map the terrestrial land cover of the globe at 1 km resolution, and a land-cover change product that will detect areas of change and identify the type of change process occurring. Land cover and both human and natural alteration of land cover, play a major role in global-scale patterns of climate and biogeochemistry of the Earth system. The importance of the physical characteristics of land cover, and the changes in these characteristics that human activities induce, have been widely recognized as key elements in the study of global change (Townshend *et al.* 1991).

Uses of the MODIS land cover product range from relatively simple biophysical parameterizations for global models to highly refined definitions of vegetation communities for change detection and socioeconomic analyses. Because of this broad array of uses we plan a two step hierarchically related product. The first step will be a simple, entirely remote sensing based product automated for global implementation at launch and designed for parameterizing global models (figure 6, Running *et al.* 1994). The second step will expand these first six classes by relying on ancillary climate, topography and landuse data, to produce refined definitions of land cover and enhanced evaluation of land cover change. This final land cover will better represent true vegetation complexity, such as different canopy heights and structures, variable vegetation densities, and multi-storied ecosystems like tree-over-grass savannahs.

The first step logic is (1) based on simple, observable, unambiguous characteristics of vegetation structure that are important to ecosystem biogeochemistry and can be measured in the field for validation, (2) remotely-sensible so that monthly global re-classifications of existing vegetation will be possible, and (3) directly translate into biophysical parameters of interest by the global climate and biogeochemical models. We plan a complete global vegetation classification derived from combinations of three primary attributes of plant canopy structure. These attributes are (1) permanence of aboveground live biomass, (2) leaf longevity, and (3) leaf type (figure 6). Possible combinations of these three vegetation attributes yield only six fundamental vegetation classes, although they occur across a range of climates (Running *et al.* 1994).

The first criteria of the classification defines whether the vegetation retains perennial or annual aboveground biomass, a critical question for seasonal climate and carbon balance modelling. This class separates vegetation with permanent respiring biomass (forests and woody stemmed shrubs) from annual crops and grasses. The next step of the classification, leaf longevity, effectively evergreen versus deciduous canopy, is an extremely critical variable in carbon cycle dynamics of vegetation, and is important for seasonal albedo and energy transfer characteristics of the land surface. This leaf longevity class defines whether a plant must completely

regrow its canopy each year, with direct consequences to ecosystem carbon partitioning, leaf litterfall dynamics and soil carbon pools. The third classification criteria defined is a simple leaf type or shape. Based on both the spectral/optical properties of leaves and their gas exchange characteristics, we suggest only three leaf types need to be defined, needleleaved, broadleaved, and grasses. The needleleaved and grass classes are fairly straightforward representations of those vegetation types, however the broadleaf class includes trees, shrubs, herbs and crops that fit this leaf type criteria. Hence, the third criteria requires the sequential solution of the first two criteria (perennial/annual, and evergreen/deciduous) to provide meaningful discrimination of vegetation.

The second step of the land cover product will provide a substantially more specific definition of land cover characteristics for multiple uses (Loveland *et al.* 1991). An external global climate database will be required in EOSDIS for separation of vegetation covers that are similar physiognomically as defined by our step one land cover, but exist in different climates. For example, climate effectively discriminates boreal from temperate forests that may be indistinguishable spectrally. Annual global climate data will be used to derive sub-class designations of tropical/temperate/boreal vegetation from the six biome types from the step 1 land cover (Prentice 1990, Prentice *et al.* 1992, Neilson *et al.* 1992).

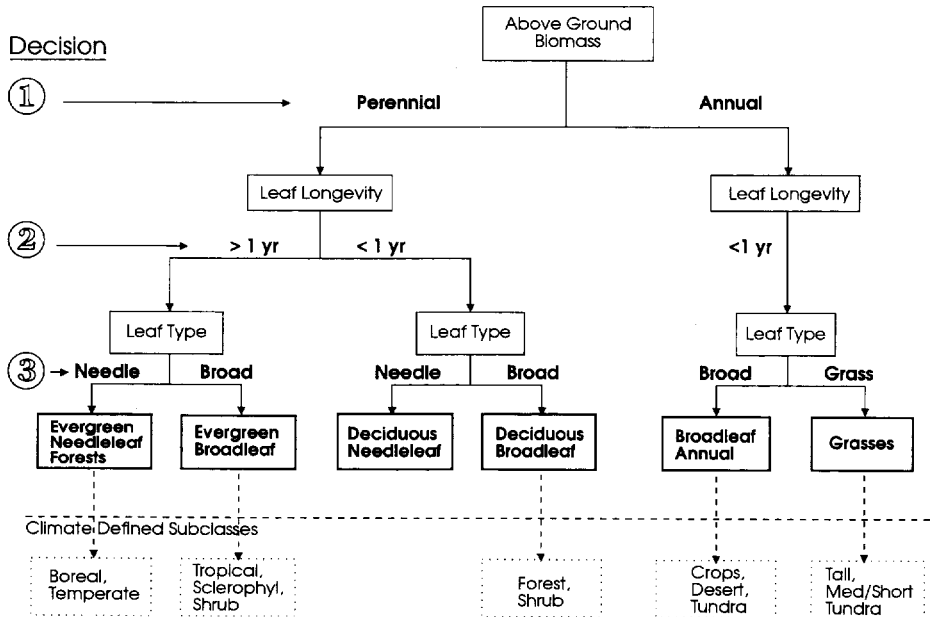


Figure 6. A flowchart of global vegetation classification logic planned for the simple step one land cover definition. Each box identifies the variable being defined, and each decision point is numbered. The final six classes of vegetation are shown in bold. Below the dotted line some potential climate-defined subclasses corresponding to more common classification schemes are suggested (from Running *et al.* 1994).

The land cover and land-cover change products will both use MODIS data in a per-pixel multiyear temporal history, to be acquired at 1 km spatial resolution. Primary MODIS inputs will be vegetation indices from the 250 m and 500 m bands, and land surface temperature at 1 km obtained from MODIS thermal bands. Also essential will be MISR derived BRDF data and digital terrain data.

The land-cover classification logic will work from a training library of time-trajectories and ancillary data that characterize the land cover types within geographical and climatological regions (figure 7(a)). A profile filter will screen noise from time-sequential measurements and provide smoothed data for parameterization of time-trajectory shapes. A 'geometry' filter will identify measurements made at viewing positions that are undesirable due to long atmospheric path lengths or BRDF effects. A texture filter will measure spatial variability in the 250 m bands and use this as a feature quantifying the spatial structure of each land cover type.

The land-cover change product will detect and categorize land-cover change processes on a global scale and quantify the rate of change. The land-cover change detection algorithm will be independent of the land-cover product, since the change detection approach does not use a simple comparison of successive land-cover maps (Townshend *et al.* 1992). The method will be based on a comparison, on a pixel-by-pixel basis, of the temporal development curve of a set of biophysical and spatial indicators derived from MODIS data, such as vegetation index, surface temperature, spatial structure, snow cover, and fire. The seasonal dynamic of these indicators will be represented by a point in a multi-dimensional space, with each dimension of this space corresponding to a time-composited observation. Change of accumulated value and seasonal dynamic of the indicator between successive years will be quantified by a distance measurement between successive points in the temporal multi-dimensional space.

For every pixel for which a significant change is detected at the MODIS resolution, two further analyses will be conducted (figure 7(b)): (1) the quantification of the change intensity, using finer spatial resolution data from other sensors (e.g., MISR, ASTER, Landsat, SPOT) as available; and (2) the categorization of the change process. This last step will be based on information provided by the land-cover product and on ecological models of vegetation succession and anthropogenic disturbance. This approach will be developed using multi-temporal AVHRR 1 km data over areas of active land-cover change in monitored ecosystems.

An important element in developing and validating the land cover and land-cover change products is a network of global test and monitoring sites, selected to be broadly representative of the global range of land covers. At each of the test sites, a multiyear temporal sequence of high resolution imagery (Landsat-MSS, TM and/or SPOT) will be combined with ground maps and data to establish a land cover database within a region of at least 100 km by 100 km.

5.3. MODIS Vegetation Indices (MVI)

The MVI are critical precursor variables for a number of advanced MODLAND products, including global land cover, terrestrial carbon and hydrologic balances, leaf area index (LAI), fraction absorbed photosynthetically active radiation (FPAR), net primary production (figure 2), and in numerous EOS interdisciplinary studies.

5.3.1. Characteristics of MODIS Vegetation Indices

Vegetation indices are dimensionless, radiometric measures usually involving reflectances from the red and near-infrared (NIR) portions of the spectrum. They

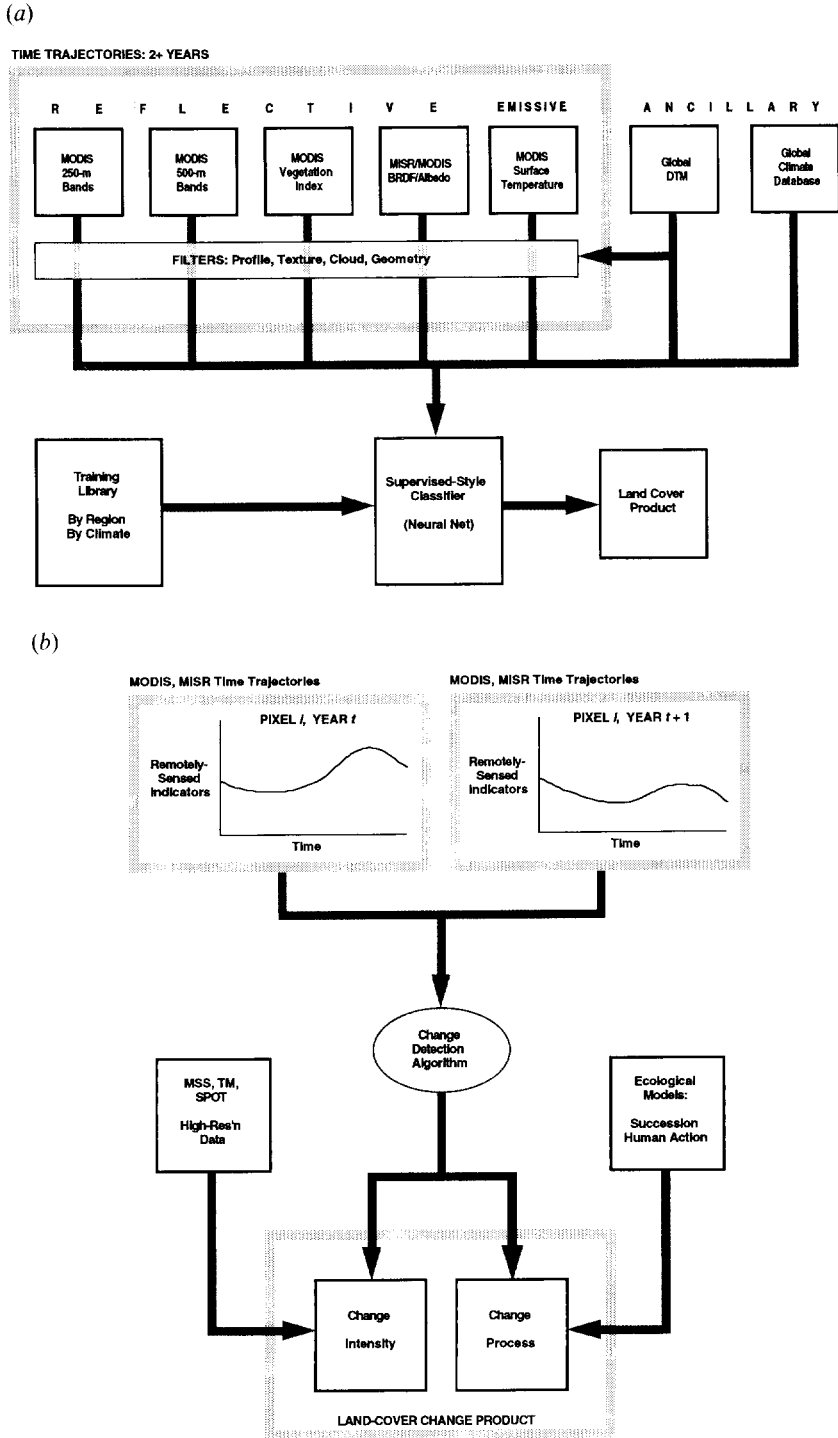


Figure 7. (a) Flow chart of the logic and components required to produce the comprehensive MODIS Land Cover algorithm. (b) Illustration of the time trajectory analysis planned for the Land Cover Change algorithm. (Provided by A. Strahler).

serve as indicators of relative abundance and activity of green vegetation, having been related to leaf area index, percentage green cover, green biomass, and FPAR (Asrar *et al.* 1984, Sellers 1985, Justice *et al.* 1985, Running *et al.* 1989, Goward *et al.* 1991).

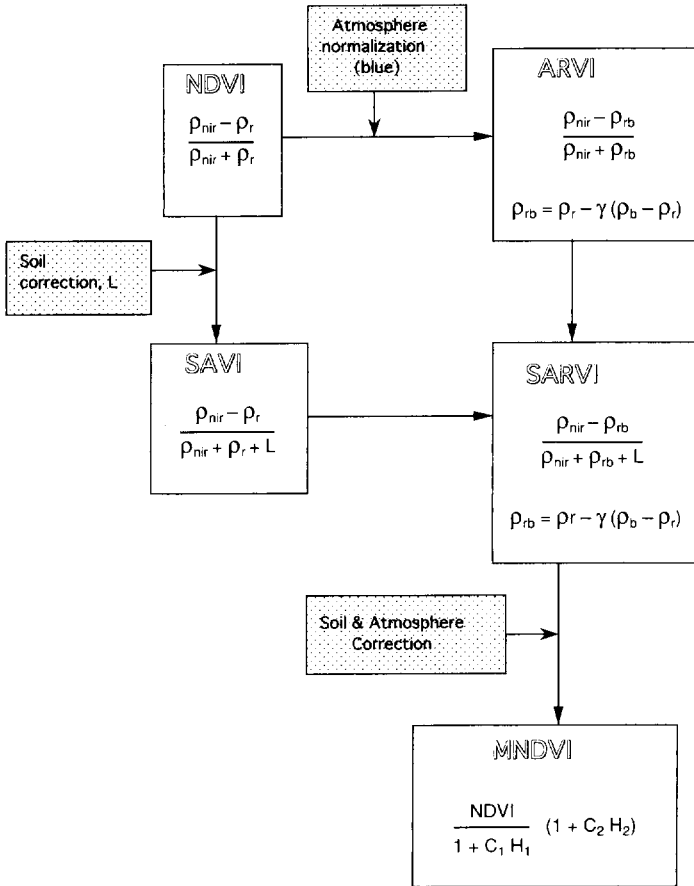
The criteria for definition of a vegetation index includes:

- (a) The index should maximize sensitivity to plant biophysical parameters, preferably with a linear response in order that sensitivity be available for a wide range of vegetation conditions, and to facilitate validation and calibration of the index.
- (b) The index should normalize or model external effects such as Sun angle, viewing angle, and atmosphere.
- (c) The index should normalize internal effects (ground contamination) such as canopy background variations, topography, and differences in senesced or woody vegetation (non-photosynthetic components of a canopy).
- (d) The index should be a global product, allowing precise and consistent spatial and temporal comparisons of vegetation conditions.
- (e) The index should be coupled to some specific, measurable biophysical parameter such as LAI or FPAR as part of the validation effort and quality control.

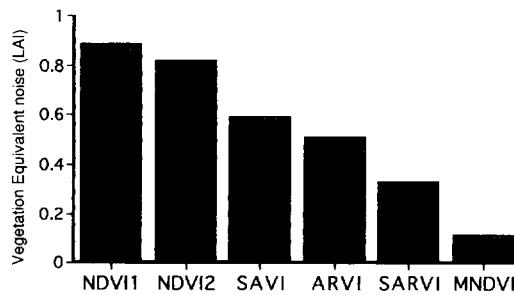
5.3.2. *Vegetation Index products for MODIS*

The current generation of global land and vegetation analysis was created primarily by NDVI products from the AVHRR, and has revolutionized global science in a time period of only ten years (Justice *et al.* 1985, Tucker *et al.* 1985, Goward *et al.* 1991). As our understanding of both the AVHRR sensor, and the NDVI algorithm has advanced, several different VIs have recently been developed and new versions of existing indices have been proposed to solve problems that have been identified (Huete 1988, Pinty and Verstraete 1992, Kaufman and Tanré 1992). The new indices are based on improved knowledge of atmospheric effects, soil effects, Sun and view angle effects, surface anisotropy, and canopy radiant transfer models. However, there remains a need to maintain long-term global data sets that are comparable with the original NDVI datasets, as well as develop improved measures of vegetation. For this reason, three types of MODIS VIs are proposed here, all intended for the general scientific community with global applicability.

- (1) Continuity Index: The NDVI, which has been the focus of a considerable amount of research to date, will become the continuity index. The MODIS NDVI will not be identical to that derived from the NOAA/AVHRR instrument due to different sensor characteristics, MODIS channels have narrower bandwidths, for example. However, continuity in the NDVI is seen as a way of extending the MODIS data record back 16 years, to the beginning of AVHRR acquisition in 1981. The exact relationship of the MODIS NDVI with the AVHRR NDVI will be established from parallel acquisitions after EOS launch.
- (2) MODIS Improved Indices: Although the NDVI has been shown useful in estimating many vegetation properties, many important external and internal influences restrict its global unity. Improved vegetation sensitivity is achieved via advanced MODIS sensor characteristics and from the optimal utilization of MODIS sensor wavebands. Figure 8(a) summarizes many of the concepts



(a)



(b)

Figure 8. (a) Relationships among the current NDVI and vegetation index variations that correct for influences of soil background and atmospheric transmissivity. SAVI=Soil Adjusted Vegetation Index, ARVI=Atmospherically Resistant Vegetation Index, SARVI=Soil and Atmospherically Resistant Vegetation Index, MNDVI=Modified NDVI. C_s and C_a are soil and atmospheric calibration terms, respectively and L_s and L_a are accompanying adjustment factors. (b) Comparisons of combined soil and atmospheric VI noise (VEN) for the AVHRR (NDVI1), MODIS (NDVI2), and MODIS Vegetation Index variants using SAIL model simulations with vegetation data from a desert cedar community. (From Huete *et al.* 1993).

introduced in the development of an improved and 'stable' vegetation index equation. As can be seen, the improved variants to the NDVI equation attempt to either incorporate a soil adjustment factor or a blue band for atmospheric normalization. The soil adjusted vegetation index (SAVI) introduced a soil calibration factor, L , to the NDVI equation to minimize soil background influences resulting from first order soil-plant spectral interactions (Huete 1988, Huete *et al.* 1992). Qi *et al.* (1994) developed a modified SAVI (MSAVI) that utilizes an iterative, continuous L' function to optimize soil-adjustment and increase the dynamic range of the SAVI.

The atmospherically-resistant vegetation index (ARVI) incorporates the blue band into the NDVI equation to stabilize the index to temporal and spatial variations in atmospheric aerosol content (Kaufman and Tanré 1992). The ARVI utilizes the difference in radiance between the blue and red channels to correct radiance in the red channel and thus reduce atmospheric influences. This index requires prior corrections for molecular scattering and ozone absorption. One may integrate the L' function in the SAVI with the blue band normalization in the ARVI and derive the soil and atmospherically resistant vegetation index (SARVI), which would correct for both soil and atmospheric noise. Lastly, a feedback based method is being developed to account for interactive atmospheric and soil noises, producing a stable or modified NDVI (MNDVI; figure 8(a), where H_1 and H_2 are soil and atmospheric feedback terms and C_1 and C_2 are accompanying adjustment factors).

The development of improved MVIs will (1) integrate more channels, particularly the blue for atmospheric correction; (2) integrate the important features of several current vegetation indices into a single index; and (3) retain the option to provide for a second functionally related MVI for extraction of additional vegetation information.

5.3.3. Post-launch experimental indices

The experimental VIs include algorithms currently in the early stages of development that may yield considerable improvement over existing VIs. For example, as the BRDF global data set and Land Cover product become more complete, it will become easier to insert surface anisotropy information for each land cover type into the satellite derived VI algorithm.

Another index plans to combine MODIS and POLDER (Polarization and Directionality of Earth's Reflectances) data to generate a vegetation index that is 'minus specular' or excluding the effects of specular light which contains no cellular pigment information. This specularly corrected Vegetation Index should be much better correlated with canopy photosynthetic capacity, which will allow improved terrestrial carbon budgets to be produced (Rondeaux and Vanderbilt 1994). The use of mixture modelling to isolate and extract the green component of an image is also being investigated.

Lastly, a systems analysis method is being developed in which interactive atmospheric and soil noises feed back to the NDVI to produce a stable, modified NDVI equation (MNDVI; figure 8(a)), where C_g and C_a are soil and atmospheric calibration terms, respectively and L_s and L_a are accompanying adjustment factors. VIs that can be directly inverted into biophysical vegetation variables such as LAI and FPAR are planned (figure 9).

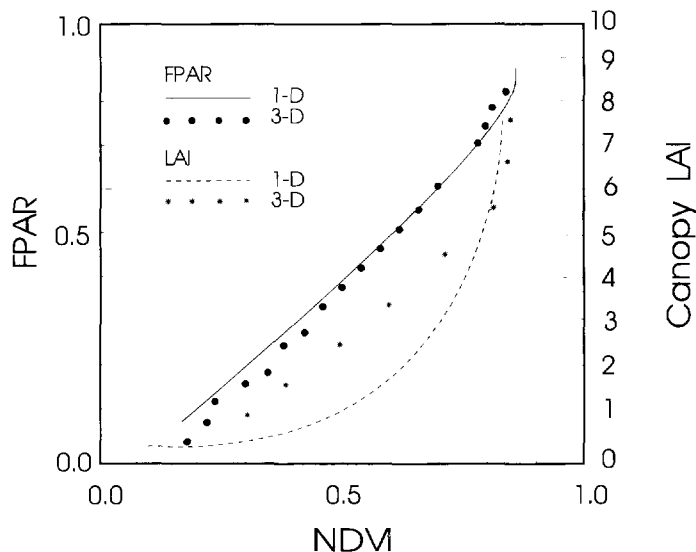


Figure 9. Theoretical relationships found between NDVI and fraction of absorbed photosynthetically active radiation (FPAR), and leaf area index (LAI). Based on both one-dimensional and three-dimensional canopy radiation simulations from Asrar *et al.* (1992). This illustrates the potential to derive advanced biophysical variables from MODIS Vegetation Indices.

5.3.4. MVI accuracy assessment

The VI products implemented for EOS will require validation with appropriate estimates of accuracy. These indices will have to be validated in both a radiometric as well as biophysical sense, requiring the establishment of selected test sites that cover a diverse range of global biomes. These data sets should include ground, air, and satellite radiometric observations accompanied by atmospheric measurements and ground vegetation sampling. As part of the validation effort, the VI response to subtle vegetation changes will be analysed amidst temporal and spatial variations attributed to canopy background, atmosphere, and Sun-view geometry.

An example of noise and uncertainty in the VI's is presented in figure 8(b). A sensitivity analysis was done with the SAIL canopy model and Lowtran atmospheric simulations run using data from a desert cedar community, with LAI's from 0 to 3, five soil backgrounds, and four atmospheric aerosols (5 km to 100 km visibilities) as conditions for comparisons of combined atmospheric and soil related noise on VI's. The vegetation equivalent noise (VEN) provides a measure of VI uncertainty in predicting LAI,

$$VEN = (VI_p - VI) / I(LAI), \quad (1)$$

where $I(LAI)$ is the slope, $dVI/dLAI$, of the VI-LAI curve at specific LAI's, VI is the true VI value, and VI_p is the perturbed VI value. The AVHRR NDVI noise exceeds that of the MODIS simulated NDVI due to the water vapour sensitivity in the AVHRR channel 2 band. All NDVI variant equations outperform the NDVI by reducing atmospheric and/or soil background variations on the VI, with the MNDVI reducing noise by nearly a factor of 10 (figure 8(b)).

Although the VI is dimensionless, an important component of validation concerns the relations between the VI and key surface biophysical parameters. Remotely-sensed radiometric measurements will be coupled with point-based biophysical measurements of LAI and FPAR over different reference land cover types. The improved MODIS VI products will be spatially and temporally averaged in compositing routines to generate higher order, cloud-free vegetation index maps on a decadal and monthly basis over a suit of spatial resolutions from 250 m to the 10 km by 10 km grid cell. The compositing algorithm will differ from the current maximum value compositing (MVC) approach and will consider land cover specific, directional sun-target-sensor interactions. MODIS will be radiometrically calibrated on an absolute scale for multi-sensor comparisons and on a relative scale, allowing temporal analyses to produce the VI's.

5.4. Snow and ice cover

Regular evaluation of terrestrial snow and ice cover is important because snow dramatically influences surface albedo, hydrologic properties, and regulates some ecosystem process activity (Robinson *et al.* 1993). Global climate models use very sensitive to the seasonal albedo shift caused by snow cover. Ecosystem models use the snowmelt period to define the onset of vegetation growing seasons, accelerate seasonal biogeochemical cycling, and trigger certain trace gas emissions. Annual hydrologic activity of many regions is dominated by the seasonality of snowpack accumulation and snowmelt.

MODIS data will be used to monitor the dynamics of snow and ice cover globally. More specific objectives are: (1) to observe and quantify the temporal and spatial variability of snow and ice cover on a hemispheric, continental and large region/watershed basis using MODIS; (2) to map the spatial, temporal and spectral variability in reflected and emitted radiances observed by MODIS over snow and ice-covered areas, and relate these observations to components of the surface radiation balance; and (3) to understand how the spatial and temporal variability in snow cover and radiation fluxes relate to surface water balance components over continental-scale drainage basins.

The approach will consist of developing and applying algorithms to identify and map snow and sea-ice cover globally, at regular time intervals (Foster *et al.* 1993). Development of the algorithms has begun over high latitude test sites using Landsat Thematic Mapper (TM) satellite data and MODIS Airborne Simulator (MAS) data (Chang *et al.* 1990). The algorithms will be tested over progressively larger regions until they can be applied globally. Active and passive microwave data will be used along with visible and near-infrared data to map snow cover and snow depth when feasible. In addition spectral reflectance and thermal properties of snow will be measured to improve our understanding of the energy balance of a snowpack and for input into models that will be used with MODIS data to calculate and map snow reflectance.

Critical remote sensing data required for studying the energy balance of a snowpack include snow cover, snow depth and snow albedo. Snow albedo is not the precise quantity measured by satellite sensors because sensors collect only a small portion of the energy scattered by the snow, specifically only that energy directed toward the sensor, and only in discrete bands or channels (Hall *et al.* 1990, 1992). The snow albedo is all energy scattered in all directions over all portions of the reflective part of the spectrum. The snow bi-directional reflectance distribution

function (BRDF) must be known for best interpretation of satellite measurements of snow reflectance. This BRDF, available from MISR data, should enable the snow albedo to be calculated. Ultimately, visible, near-infrared, thermal infrared and microwave data will be used in concert to map snow cover, depth and albedo globally in the EOS era.

5.5. Land surface temperature

Accurate land surface temperature (LST) algorithms are required for a wide variety of climate, hydrologic, ecological and biogeochemical Earth processes studies. LST is the emitted longwave radiation component of land surface energy balances. Hydrologic processes such as evapotranspiration and snowmelt are highly sensitive to surface temperature fluctuation. Ecological processes of growing season leaf phenology, photosynthesis, respiration, and decomposition are also especially sensitive to surface temperature. Recent research is finding that the addition of LST can effectively discriminate regional land cover classes more effectively than NDVI data alone (figure 10).

The accuracy specification for MODIS LST algorithms is 1–3°C (1°C in the 0–5°C range). LST is much more difficult to estimate from satellite measurements than sea surface temperature (SST) because land-surface properties and conditions such as emissivity are much more heterogeneous. Global SST ranges from 0–30°C,

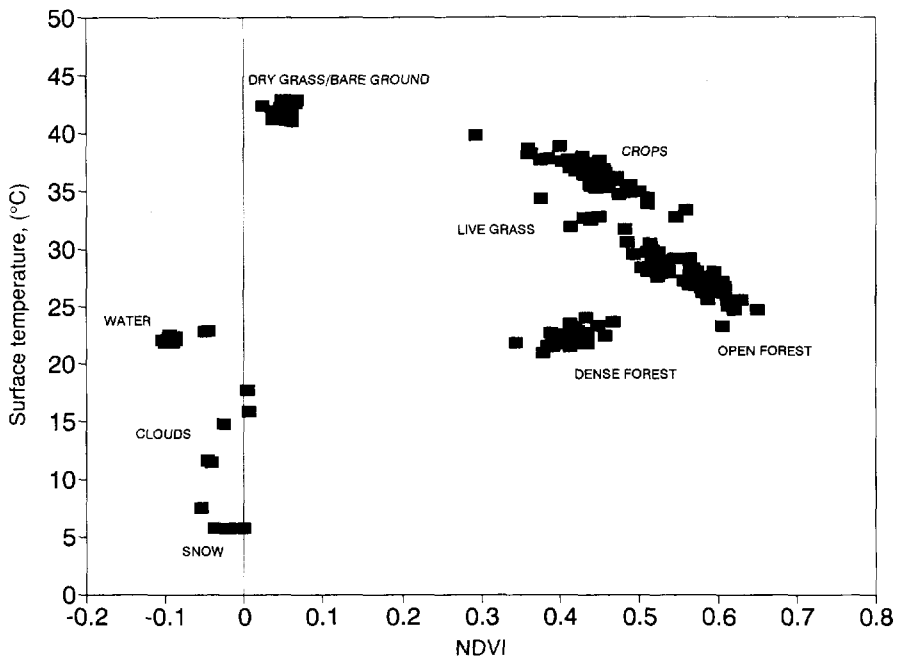


Figure 10. An example of use of land surface temperature (LST) to provide additional separation of land cover types. From a 512 km by 512 km scene of western Montana, AVHRR data for 14 June 1985. Note the clustering of land cover classes between NDVI of 0.3–0.6, and the improved discrimination possible after adding a Y-axis of LST. (Provided by R. Nemani).

while the range of natural LST is from -50 to $+60^{\circ}\text{C}$, with fire and volcanic activity having much higher surface temperatures. Additionally, LST can vary 20°C diurnally at one point, or an equal magnitude instantaneously within a few square kilometers of land area. Computational considerations for the LST must consider spectral variations in surface emissivities and reflectivities of various land covers, wide variations of surface moisture, topographic variability, atmospheric profile variations in the boundary layer, a much larger range of potential surface temperatures, and 'mixed-pixel' problems resulting from micro-scale temperature heterogeneity. Therefore, more thermal bands have to be used in LST algorithms (Wan and Dozier 1989), and temporal frequency is important.

In the medium wavelength infrared range from 3.5 to $4.1\ \mu\text{m}$, the solar radiation scattered by the atmosphere and reflected by land surfaces is always comparable to or larger than surface thermal emittance. Therefore, an accurate solar correction model must be developed in order to estimate surface temperature by using daytime MODIS thermal infrared data in this wavelength region.

Although a wealth of temperature data are available from existing meteorological stations, these data are normally a near-surface air temperature for a single point, not a radiometric skin temperature of a multi-kilometer area. Also few *in situ* LST data are available to allow investigation of the inherent difficulties in ground-based LST measurements from surface heterogeneity or canopy structure and topographic shadowing. Consequently, the LST algorithm will mainly depend on accurate radiative transfer simulations. The accuracy of simulation results depends on the methods used for solving the atmospheric radiative transfer problem and our knowledge of temperature dependent atmospheric molecular absorptions. Accurate SST and LST algorithms rely on increasing accuracy of molecular absorption measurements at different pressures in a wide temperature range from 200 – $300\ \text{deg K}$. Direct quantitative comparisons between satellite thermal infrared data and *in situ* spectral radiometric measurements of emissivity-known surfaces (such as sea and lake surfaces), combined with atmospheric radiosonde data will provide a means to evaluate the accuracy of molecular absorptions and to validate radiative transfer simulations and algorithms.

Sufficient knowledge of spectral emissivity and reflectivity characteristics of various land cover (including canopy and soils) must be gained in the next few years by accurate laboratory and field measurements so that LST algorithms can be developed. Based on experiences from evaluating SST algorithms, a practical multi-band LST hierarchical algorithm will be developed, that will incorporate regional and seasonal characteristics, viewing angle and topographic effects, and land cover grouping according to spectral emissivity and reflectivity features.

5.6. Fire

Fire has played a critical role in the development of existing patterns of global vegetation and continues to be an important process in several major biomes. In the boreal forest regions it is a primary agent in forest succession. In the tropics, fire plays an integral role in savanna ecosystem functioning and nutrient cycling and is used extensively for agriculture. Fire is also a major source of trace gases and particulates to the atmosphere (Crutzen and Andreae 1990). Current estimates of trace gas emissions from biomass burning are severely constrained by the lack of reliable statistics on fire distribution and frequency, accurate estimates of area burned, fuel load and fuel moisture content. Modelling of atmospheric transport

and chemistry requires knowledge of the distribution and timing of fires and their associated emissions.

Existing satellite sensing systems provide the basis for developing the requirements for the MODIS fire detection capability and are summarized by Justice *et al.* (1993). The AVHRR is considered the precursor instrument for MODIS fire detection with similar spatial and temporal resolution. The middle infrared ($3.7\ \mu\text{m}$) and thermal channel ($10.8\ \mu\text{m}$) of the NOAA AVHRR series provides the means to detect active flaming fires. The low saturation level of the middle infrared channel of 320 K provides a major constraint to the measurement of fire size and temperature. The visible and near-infrared channels of the AVHRR permit the direct identification of burn scars, and the monitoring of vegetation state (Lopez *et al.* 1991, Paltridge and Barber 1988, Kasischke *et al.* 1993).

The current instrument design for MODIS fire detection includes high saturation bands at $3.95\ \mu\text{m}$ and $11.03\ \mu\text{m}$ with a 1 km resolution, and bands at $1.6\ \mu\text{m}$ and $2.13\ \mu\text{m}$ at 500 m resolution (see table 2). In addition there is the possibility of nighttime fire detection using the $0.845\ \mu\text{m}$ band at 250 m resolution. These bands will permit the measurement of fire size and temperature. The MODIS visible and near-infrared bands with their high spatial resolution, will also permit the improved detection of fire scars over the current capability of the AVHRR. The MODIS fire products available at-launch will provide daily estimates of active fire occurrence, size and temperature. Additional post-launch development will lead to estimates of burned area, which when combined with estimates of vegetation cover and standing biomass would provide the basic inputs to trace gas emissions models.

5.7. Biophysical variables

A number of biophysical parameters are also required for use in advanced global models of climate, hydrology, biogeochemistry and ecology, and were requested by many of the EOS Interdisciplinary Projects. These variables describe vegetation canopy structure, and are related to functional process rates of energy and mass exchange.

Leaf area index (LAI), a canopy structural variable, and fraction of absorbed photosynthetically active radiation (FPAR), a radiometric variable, have both been related directly to the NDVI from AVHRR by theoretical canopy modelling (see figure 9 and Sellers 1985, Asrar *et al.* 1992) and field studies (Asrar *et al.* 1984, Nemani and Running 1989). First Kumar and Monteith (1981) and then Asrar *et al.* (1984) showed that absorbed PAR (APAR) may be estimated by remote sensing. NDVI is about equal to the Fraction of PAR that is absorbed (FPAR):

$$FPAR = APAR/PAR \approx NDVI \quad (2)$$

(Asrar *et al.* 1984). However, Gutman (1991), Goward and Huemmrich (1992) and Asrar *et al.* (1992) demonstrated problems with using NDVI for estimating FPAR. The new MODIS Vegetation indices will overcome problems from atmospheric effects and background soil reflectance, and produce improved estimates of FPAR.

Both LAI and FPAR have been used extensively as satellite derived parameters for calculation of surface photosynthesis, evapotranspiration and net primary production (Sellers 1985, Running 1990, Prince 1991). Appropriate MODIS Vegetation Indices, and the conversion functions to estimate LAI and FPAR for different biomes of varying canopy structure will be developed by MODLAND for EOS research.

Roughness length is a vegetation structural parameter used in climate models for calculating energy transfer and surface drag, or momentum transfer. We plan that a reasonable estimate of roughness length will be produced first from MVI, later improved with global BRDF information, as a post-launch product.

Surface resistance, the resistance of a surface to water vapour transfer, is a fundamental measure of drought and will have immense practical utility for crop production, fire danger, and hydrologic discharge models. Current logic for a satellite derived surface resistance uses a combination of NDVI and surface temperature, a good example of synergism of the MODIS products. Development of this product has been with AVHRR data to date, and has covered only regional areas because of computational loads (Goward *et al.* 1985, Hope 1988, Nemani and Running 1989, Nemani *et al.* 1993). A surface resistance algorithm derived from MVI and MODIS LST is planned as a post-launch product, and is an essential precursor to the global evapotranspiration product.

5.8. Terrestrial Ecology Products

MODLAND products will be used to generate a number of advanced ecosystem process algorithms. A weekly biome specific terrestrial photosynthesis (PSN) for the globe is scheduled as an at-launch product, and weekly evapotranspiration (ET) as a post-launch product (Running 1990). These new global products will require biome definition based on land cover, growing season phenology from the MVI, and ecosystem process rates for photosynthesis, respiration, evapotranspiration and decomposition utilizing biome simulation models (figure 11).

Theoretically, instantaneous PSN can be approximated by PAR absorbed and a conversion efficiency. This logic has been adapted to remote sensing and global applications by using AVHRR/NDVI as an estimate of FPAR:

$$PSN \approx (NDVI)(PAR)\varepsilon \quad (3)$$

where ε is a PAR conversion efficiency from energy to dry matter (g/MJ). We plan for MODIS an explicit use of this logic that separates meteorological from biochemical controls of vegetation canopy mass and energy exchange.

$$PSN = (MVI)(PAR)\varepsilon_c \quad (4)$$

produced from the weekly composited MVI. The time summation of PSN through the growing season gives an estimate of NPP, the annual sum being:

$$NPP = \Sigma(MVI)(PAR)\varepsilon_c \quad (5)$$

where:

NPP = net primary production, kg C km⁻² yr⁻¹

ε_c = biome specific conversion factor from FPAR to carbon NPP, gC(MJ)⁻¹

A mechanistic ecosystem process model, BIOME-BGC is used to derive biome specific ε_c values (Running and Hunt 1993, Hunt and Running 1992). Following Prince (1991), an expanded analysis of the PAR carbon conversion efficiency is:

$$\varepsilon_c = \varepsilon_{max}(f)(Y_g)(Y_m) \quad (6)$$

where ε_{max} is the maximum ε possible ($\varepsilon_{max} \approx 2.7$ gC mJ⁻¹), f is the fraction of the growing season available for photosynthesis, primarily controlled by cold air

temperatures and seasonal drought, Y_g is the fraction of photosynthesis consumed by growth respiration (about 30 per cent), and Y_m is the fraction of photosynthesis consumed by maintenance respiration (about 25 to 40 per cent). The fraction f is primarily determined by climate, where Y_g and Y_m are primarily determined by lifeform.

Seasonal evapotranspiration can be approximated globally with similar logic, using a partitioning of energy absorbed to potential evaporation, ϵ_w , and restricting actual evaporation with a surface resistance:

$$ET = \Sigma(\sigma(MVI)(PAR))\epsilon_w \quad (7)$$

where:

ET = evapotranspiration, kg day

ϵ_w = reciprocal of latent heat of vapourization, 0.41 kg MJ^{-1}

σ = surface resistance, day^{-1}

These formulations should be generally applicable under a wide variety of climatic conditions and biome types because climate is considered explicitly, and varying biome types are defined by the MODIS land cover product and represented

TERRESTRIAL PRODUCTIVITY MODIS PRODUCTS AT LAUNCH

Inputs from EOSDIS

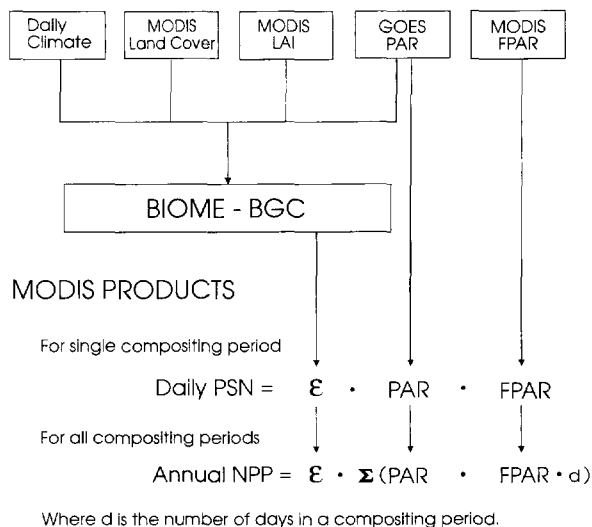


Figure 11. The planned integration of initial MODLAND products with advanced biome biogeochemical models BIOME-BGC, to produce global carbon and hydrologic balances. Six different versions of the biome model will be used, one for each of the simple land cover classes in figure 6. The models will produce biome specific, seasonally dynamic conversion efficiency coefficients ϵ_c for carbon and ϵ_w for water fluxes. (From Running and Hunt 1993).

by biome specific ϵ factors. As MODIS airborne simulator (MAS) data, and the MODIS data become available, the AVHRR based NDVI used during development of these products will be replaced with the improved MVI.

We then plan at-launch to produce weekly, biome-specific net photosynthesis of the global terrestrial biosphere (figure 12) at 1 km spatial resolution, from the weekly composited Σ MVI, and annual global terrestrial primary production. These carbon balances will quantify both temporally and spatially the sources and sinks of terrestrial CO₂ globally. The global ET product relies on the surface resistance to represent drought conditions that biologically constrain surface evaporation. Because surface resistance is a post launch product, global ET will also not be available until post-launch. The weekly global ET will provide the hydrologically controlled energy partitioning necessary for surface parameterization of the global climate models.

6. Validation strategy

The first step in MODLAND product validation will be a formal peer review process for the logic and concept of these algorithms. Normal journal review procedures occur for these products when presented in journal articles, and the references cited here illustrate the considerable amount of publication in journals of the MODLAND algorithm development to date. A next level of on-going review is from other members of the EOS science community, followed by external peer review panels.

For field validation, the strategy for algorithm development and land product validation is to identify a network of the 60–70 global test sites, about 100 km by 100 km in size, for which we will assemble AVHRR, MSS, TM, and/or SPOT data sets. These sites will be chosen where international collaborators can provide ground information about the biological and physical characteristics of the region.

6.1. Baseline test sites

The development of MODIS land algorithms will require a combination of both regular monitoring and intensive field measurements. Consequently the MODLAND team currently plans to recruit test sites for both short and long term activities. Ongoing monitoring activities will best be accomplished by an existing, organized network of study sites already established to provide monitoring of terrestrial variables. A number of site networks already exist, the most prominent of which is the U.S. National Science Foundation Long Term Ecological Research network of 19 study areas distributed throughout the United States, representing a variety of biome types from forest to grasslands to tundra. Internationally, the U.N. Man and Biosphere program has identified Biosphere reserves around the world, and the International Geosphere-Biosphere Program plans a Global Terrestrial Observation System (GTOS) (Brian Walker, personal communication).

Data needed by MODLAND from land monitoring sites would include for example, the following:

1. A land cover map, updated every five years, documenting change.
2. Leaf area index map, possibly done seasonally.
3. Net primary production and standing biomass.
4. Daily surface meteorology, including surface temperature.
5. Weekly snow cover and snowmelt.

6. Soil surface wetness and moisture depletion.
7. Hydrologic discharge from gauged watersheds.
8. Fire activity, coverage and duration.
9. Sun photometer data.

6.2. *Multi-sensor Aircraft Campaigns, MACS*

In addition to regular monitoring, occasional major campaigns bring together a variety of scientific disciplines necessary to explore critical theoretical questions on terrestrial remote sensing and land-atmosphere interactions. These projects typically mobilize a suite of measurements from ground base, towers, aircraft and satellites, and incorporate a strong database organization and simulation modelling synthesis. The FIFE experiment in Kansas (Sellers *et al.* 1988), HAPEX-MOBILHY in France (Andre *et al.* 1988), HAPEX-Sahel (Prince 1991), and OTTER programme in Oregon (Peterson and Waring 1994) are recent examples of major multi-disciplinary campaigns. The joint NASA-Canada supported BOREAS experiment scheduled for 1993-94 in central Canada is the next major project planned. Future projects in other major biome types, such as tropical forests in the Amazon Basin are under consideration.

6.3. *PATHFINDER datasets*

'Pathfinder' is the term that has been applied to a new generation of Earth sciences data sets developed for the study of global environmental change (Maiden 1994). Pathfinders take advantage of the history of satellite observations beginning in 1971 for Landsat, and 1981 for AVHRR that are available in currently existing archives.

6.3.1. *AVHRR Pathfinder*

In general, the criteria for choosing AVHRR Pathfinder data sets include: (1) the data must provide a consistently processed global, multiple year dataset, (2) production must begin at once; (3) the products must be immediately useful to the scientific community and in an accessible media; and (4) they must not rely on research breakthroughs for production. A calibrated AVHRR Pathfinder data set, comprised of a minimum of 10-years of 5-channel, 4 km GAC-AVHRR data from NOAA-7, -9 and -11 (i.e., the *afternoon* NOAA satellites) is being produced (James and Kalluri 1994).

6.3.2. *Landsat Pathfinder*

A Landsat Pathfinder dataset is also planned, in order to maximize the scientific application of the 20 years of Landsat data. The data sets for the Landsat Pathfinder Data Archive will include: consistently processed scenes which have been radiometrically and systematically corrected; geocoded scenes (registered to a map base); multiscene mosaics; cloud-reduced composites; and co-registered triplicates consisting of three geocoded Landsat scenes. Currently, the USGS is producing Landsat data sets of South America, Central Africa, and south-east Asia for the Humid Tropical Forest Inventory Project conducted by NASA, the University of New Hampshire, and University of Maryland, and of North America for the North America Landscape Characterization Project conducted by the U.S. Environmental Protection Agency. Both projects require Landsat scenes acquired during the 1970s, 1980s, and 1990s. These data products will be used to produce derivative products

such as land cover maps and thematic images, e.g., land cover change, rates of deforestation, and NDVI.

6.4. MODIS Simulator (MAS)

An important pre-launch testbed for MODIS algorithms will be executed with the MODIS Airborne Simulator (MAS). MAS is a modified Daedalus Wildfire scanner which provides spectral information similar to the MODIS. The MAS collects high spatial resolution imagery at wavelengths from 0.55 to 14.3 μm . Fifty spectral bands are available in this range, and currently any 12 of these may be selected for recording during flight at 8-bit resolution. A data system which will record all 50 spectral bands at 12-bit resolution is under development. The MAS spectrometer is mated to a scanner sub-assembly which collects image data with an IFOV of 2.5 mrad, giving a ground resolution of 45 m from 18000 m altitude, and a cross-track scan width of 85.92°. A MAS Level-1 processing system was designed and implemented by the MODIS Science Data Support Team at GSFC during 1991, and processed the first MAS flight data in November 1991. The processing system ingests MAS aircraft sensor, engineering and navigation data, and produces calibrated, geolocated radiances in a portable format.

The MAS has participated in two field campaigns so far, the FIRE Cirrus study in November/December 1991 over the Coffeyville, Kansas field site and the Texas-Louisiana Gulf coast, and the ASTEX marine stratocumulus study in June 1992 over the mid-Atlantic Ocean. During 1993 the MAS was flown during the TOGA/COARE and CEPEX experiments in the southwestern Pacific Ocean. An Amazonian biomass burning experiment is planned for 1993–1994.

7. EOSDIS data delivery

The U.S. Geological Survey EROS Data Center (EDC) has been designated by NASA as the EOSDIS Land Processes Distributed Active Archive Center (DAAC). EDC will be responsible for archiving and distributing initial MODIS land data products, and for processing, archiving, and distributing advanced MODIS land data products as they are developed. The specifications for high level MODIS products will be guided by the development of MODIS precursor data sets, leading to an operational product generating capability at the time of launch. In the prelaunch era, advanced algorithms generated by the MODLAND team will be implemented at EDC.

The primary source for MODIS precursor data is 1 km AVHRR data. EDC receives AVHRR daily, and processing capability is centered on the development of time-series maximum NDVI composite data sets, including the radiometric calibrated, co-registered AVHRR spectral channels and associated satellite viewing geometry. EDC has been routinely producing maximum NDVI composite data sets of the conterminous U.S. (Eidenshink 1992), Alaska, Eastern Europe and the former U.S.S.R. since 1987. EDC in cooperation with the Canada Centre for Remote Sensing (CCRS), has produced a prototype 1 km AVHRR NDVI composite data set of North America, including a significant portion of the world's boreal forest, and a global 1 km data set from one date in June, 1992 (Eidenshink and Foundeen 1994).

EDC is cooperating with the European Space Agency and IGBP DIS to assemble a daily global 1 km AVHRR data set from 22 HPRT receiving stations

worldwide, for 18 months from April 1992 (Eidenshink and Foundeen 1994, James and Kalluri 1994). The global 1 km AVHRR data sets will provide the basis for testing and extrapolating the new algorithms used to develop the MODLAND core products. It is an EDC goal to produce a set of initial MODLAND products in 1994, including land cover, spectral vegetation index, surface temperature, and snow cover.

Delivery times of products are currently planned at 3 days after the data collection. Land MODIS data will be achieved at the EROS DAAC. A national high-speed computer network will then make available processed MODIS data to all users. A browse/query system is planned by EOSDIS to facilitate use of MODIS data by a wide user community. By 1996, EDC then plans to produce regular maps of MODLAND at-launch products for the global boreal forest biome as part of the BOREAS project.

Additional ancillary datasets are also planned to be part of the EOSDIS. These include global topography, global soil characteristics, global meteorology, political boundaries, population centres, etc. Clearly, a global GIS must be part of the EOSDIS framework (Asrar and Dokken 1993).

8. Science payoffs

The Earth Observing System is an expensive, ambitious science programme, yet essential to our ability to track the degree and rapidity of global environmental degradation that is a fundamental risk to global habitability. Expensive socioeconomic decisions may be necessary to solve an array of environmental problems, and these decisions will require global data with unprecedented levels of accuracy.

We envisage by 2000 an EOSDIS system whereby the MODIS sensor and MODLAND algorithms will provide highly calibrated, atmospherically corrected and georegistered global data sets continuously monitoring critical terrestrial variables. The MODIS sensor will produce radiance from more spectral channels at higher spatial resolution than any previous globally operating sensor. The most fundamental products, land-cover and advanced MODIS spectral vegetation indices, will incorporate multi-directional imaging whose accuracy of land surface definition should revolutionize global land surface mapping. The hydrologic budget algorithms will provide direct analysis of biospheric processes that will be essential components of global climate models, and the advanced carbon budget analyses will evaluate change or degradation in biospheric primary production, and greenhouse gas emissions. These MODLAND products will be available through EOSDIS to a global community of scientists and policy makers for rapid and accurate analysis of global change questions.

However, the community of scientists building these MODLAND products, as seen by the authorship of this paper, is small relative to the research and development needed for these global data sets. The MODLAND team welcomes collaboration with other global investigators in developing this new era of global science.

Acknowledgments

Funding for the U.S. MODLAND members is provided by contracts from the National Aeronautics and Space Administration, Office of Mission to Planet Earth.

Funding for Muller comes from NERC (U.K.), and for Teillet from the Canada Centre for Remote Sensing.

References

- ANDRE, J. C., and 30 others, 1988, Evaporation over land-surfaces—first results from HAPEX-MOBILHY special observing period. *Annals of Geophysics*, **6**, 477–492.
- ASRAR, G., and DOKKEN, D. J., 1993, *EOS Reference Handbook* (Greenbelt; MD: NASA).
- ASRAR, G., FUCHS, M., KANEMASU, E. T., and HATFIELD, J. L., 1984, Estimating absorbed photosynthetic radiation and leaf area index from spectral reflectance in wheat. *Agronomy Journal*, **76**, 300–306.
- ASRAR, G., MYNENI, R. B., and CHOUDHURY, B. J., 1992, Spatial heterogeneity in vegetation canopies and remote sensing of Absorbed Photosynthetically Active Radiation: a modeling study. *Remote Sensing of Environment*, **41**, 85–101.
- CEES, 1992, Our Changing Planet: The FY 1992 U.S. Global Change Research Program. Committee on Earth and Environmental Sciences (Washington, D.C.: National Science Foundation).
- CHANG, A. T. C., FOSTER, J. L., and HALL, D. K., 1990, Satellite sensor estimates of Northern Hemisphere snow volume. *Remote Sensing Letters*, **11**, 167–172.
- CRUTZEN, P. J., and ANDREAE, M. O., 1990, Biomass burning in the Tropics: impact on atmospheric chemistry and biological cycles. *Science*, **2501**, 1669–1678.
- DINER, D., BRUEGGE, C. J., MARTONCHIK, J. V., BOTHWELL, G. W., DANIELSON, E. D., FORD, V. G., HOVLAND, L. E., JONES, K. L., and WHITE, M. L., 1991, A multi-angle image spectroradiometer for terrestrial remote sensing with the Earth Observing System. *International Journal of Imaging Systems and Techniques*, **3**, 92–107.
- EIDENSHINK, J. C., 1992, The 1990 conterminous U.S. AVHRR data set. *Photogrammetric Engineering and Remote Sensing*, **58**, 809–813.
- EIDENSHINK, J. C., and FAUNDEEN, J. L., 1994, The 1 km resolution global data set: current progress. *International Journal of Remote Sensing*, **15**, 3443–3462.
- FOSTER, J. L., WINCHESTER, J. W., and DUTTON, E. G., 1994, The date of snow disappearance on the arctic tundra as determined from satellite, meteorological station and radiometric *in situ* observations. *I.E.E.E. Transactions on Geoscience and Remote Sensing*, (in press).
- GOWARD, S. N., CRUIKSHANKS, G. D., and HOPE, A. S., 1985, Observed relation between thermal emission and reflected spectral radiance of a complex vegetated landscape. *Remote Sensing of Environment*, **18**, 137–146.
- GOWARD, S. N., MARKHAM, B., DYE, D. G., DULANEY, W., and YANG, J., 1991, Normalized difference vegetation index measurements from the Advanced Very High Resolution Radiometer. *Remote Sensing of Environment*, **35**, 257–277.
- GOWARD, S. N., and HUENNRICH, K. F., 1992, Vegetation canopy PAR absorptance and the Normalized Difference Vegetation Index: an assessment using the SAIL model. *Remote Sensing of Environment*, **39**, 119–140.
- GUTMAN, G. G., 1991, Vegetation indices from AVHRR: an update and future prospects. *Remote Sensing of Environment*, **35**, 121–136.
- HALL, D. K., KOVALICK, W. M., and CHANG, A. T. C. 1990, Satellite-derived reflectance of snow-covered surfaces in northern Minnesota. *Remote Sensing of Environment*, **33**, 87–96.
- HALL, D. K., FOSTER, J. L., and CHANG, A. T. C., 1992, Reflectance of snow as measured *in situ* and from space in sub-arctic areas in Canada and Alaska. *I.E.E.E. Transactions on Geoscience and Remote Sensing*, **30**, 634–637.
- HOLBEN, B. N., ECK, T. F., and FRASER, R. S., 1991, Temporal and spatial variability of aerosol optical depth in the Sahel region in relation to vegetation remote sensing. *International Journal of Remote Sensing*, **12**, 1147–1163.
- HOLBEN, B. N., VERMOTE, E., KAUFMAN, Y. J., TANRÉ, D., and KALB, V., 1992, Aerosol retrieval overland from AVHRR data—Application for atmospheric correction. *I.E.E.E. Transactions on Geoscience and Remote Sensing*, **30**, 212–221.
- HOPE, A. S., 1988, Estimation of wheat canopy resistance using combined remotely sensed spectral reflectance and thermal observations. *Remote Sensing of Environment*, **24**, 369–383.

- HUETE, A. R., 1988, A soil-adjusted vegetation index (SAVI). *Remote Sensing of Environment*, **25**, 295–309.
- HUETE, A. R., HUA, G., QI, J., CHEHBOUNI, A., and VAN LEEUWEM, W. J. D. G., 1992, Normalization of multidirectional red and NIR reflectances with the SAVI. *Remote Sensing of Environment*, **40**, 1–20.
- HUNT, E. R. JR., and RUNNING, S. W., 1992, Simulated dry matter yields for aspen and spruce stands in the North American boreal forest. *Canadian Journal of Remote Sensing*, **18**, 126–133.
- IGBP, 1990, The International Geosphere-Biosphere Program: A Study of Global Change, The Initial Core Projects. IGBP Report #12, Royal Swedish Academy of Sciences, Stockholm, Sweden.
- IPCC, 1991, *Climate Change, The IPCC Response Strategies*, Intergovernmental Panel on Climate Change (Washington, D.C.: Island Press).
- IRONS, J., RANSON, D., WILLIAMS, D., IRISH, R., and HUEGEL, F., 1991, An off-nadir-pointing imaging spectroradiometer for terrestrial ecosystem studies. *I.E.E.E. Transactions on Geoscience and Remote Sensing*, **29**, 66–74.
- JAMES, M., and KALLURI, S. N. V., 1994, The Pathfinder AVHRR data set: an improved coarse resolution data set for terrestrial monitoring. *International Journal of Remote Sensing*, **15**, 3347–3363.
- JUSTICE, C. O., TOWNSHEND, J. R. G., HOLBEN, B. N., and TUCKER, C. J., 1985, Analysis of the phenology of global vegetation using meteorological satellite data. *International Journal of Remote Sensing*, **6**, 1271–1318.
- JUSTICE, C. O., MALINGREAU, J. P., and SETZER, A. W., 1993, Satellite remote sensing of fires: potential and limitations. In *Fire in the Environment; its Ecological, Climatic and Atmospheric Chemical Importance*, edited by P. J. Crutzen and J. G. Goldammer, Dahlem Workshop Report (Chichester: John Wiley and Sons), pp. 77–88.
- KASISCHKE, E. S., HARRELL, P., USTIN, S. L., and BARRY, D., 1993, Monitoring of wildfires in boreal forests using AVHRR Large Area Coverage imagery. *Remote Sensing of the Environment*, **44**, 51–71.
- KAUFMAN, Y. J., and SENDRA, C., 1988, Algorithm for automatic atmospheric corrections to visible and near-IR satellite imagery. *International Journal of Remote Sensing*, **9**, 1367–1381.
- KAUFMAN, Y. J., and TANDRÉ, D., 1992, Atmospheric resistant vegetation index. *I.E.E.E. Journal of Geoscience and Remote Sensing*, **30**, 261–270.
- KING, M. D., KAUFMAN, Y. J., MENZEL, W. P., and TANRÉ, D., 1992, Remote sensing of cloud aerosol and water vapor properties from the Moderate Resolution Imaging Spectrometer. *I.E.E.E. Transactions on Geoscience and Remote Sensing*, **30**, 7–27.
- KIMES, D. S., NORMAN, J. M., and WALTHALL, C. L., 1985, Modeling the radiant transfer of sparse vegetation canopies. *I.E.E.E. Transactions on Geoscience and Remote Sensing*, **GE-23**, 695–704.
- KUMAR, M., and MONTEITH J. L., 1981, Remote sensing of crop growth. In: *Plants and Daylight Spectrum*, edited by H. Smith (London: Academic Press), pp. 133–144.
- LI, X., and STRAHLER, A. H., 1992, Geometric-optical bidirectional reflectance modeling of the discrete-crown vegetation canopy: Effect of crown shape and mutual shadowing. *I.E.E.E. Transactions on Geoscience and Remote Sensing*, **30**, 276–292.
- LOPEZ, S., GONZALEZ, F., LLOP, R., and CUEVAS, J. M., 1991, An evaluation of the utility of NOAA AVHRR imagery for monitoring forest fire risk in Spain. *International Journal of Remote Sensing*, **12**, 1841–1851.
- LOVELAND, T., MERCHANT, J., OHLEN, D., BROWN, J., 1991, Development of a Land-Cover characteristics database for the conterminous U.S. *Photogrammetric Engineering and Remote Sensing*, **57**, 1453–1463.
- MAIDEN, M., 1994, The Pathfinder project. *International Journal of Remote Sensing*, **15**, 3333–3345.
- MULLER, J-P., and EALES, P., 1990, Global topography accuracy requirements for EOS. *Proceedings IGARSS 1990*, pp. 1411–1414.
- MYNENI, R., ASRAR, G., and GERSTL, S. A. W., 1990, Radiative transfer in three-dimensional leaf canopies. *Transportation Theory and Statistical Physics*, **19**, 205–250.
- NASA, 1992, MODIS-N Specifications, Goddard Spaceflight Ctr Ref #422-20-02, Greenbelt, MD 20771.

- NEMANI, R. R., and RUNNING, S. W., 1989, Estimation of resistance to evapotranspiration from NDVI and Thermal-IR AVHRR data. *Journal of Applied Meteorology*, **28**, 276-284.
- NEMANI, R. R., RUNNING, S. W., PIERCE, L. L., and GOWARD, S. N., 1993, Developing satellite derived estimates of surface moisture status. *Journal of Applied Meteorology*, **32**, 548-557.
- NEILSON, R., KING, G., and KOERPER, G., 1992, Toward a rule-based biome model. *Landscape Ecology*, **7**, 27-49.
- NILSON, T., and PETERSON, U., 1991, A forest canopy reflectance model and a test case. *Remote Sensing of Environment*, **37**, 131-142.
- PALTRIDGE, G. W., and BARBER, J., 1988, Monitoring grassland dryness and fire potential in Australia with NOAA/AVHRR data. *Remote Sensing of Environment*, **25**, 381-394.
- PETERSON, D. L., and WARING, R. H., 1994, Overview of the Oregon transect ecosystem research project. *Ecological Applications*, **4**, 211-225.
- PINTY, B., and VERSTAETE, M. M., 1992, GEMI: A non-linear index to monitor global vegetation from satellites. *Vegetatio*, **101**, 15-20.
- PRENTICE, K. C., 1990, Bioclimatic Distribution of Vegetation for General Circulation Model Studies. *Journal of Geophysical Research*, **95**, 11811-11830.
- PRENTICE, C., CRAMER, W., HARRISON, S., LEEMANS, R., MONSERUD, R., and SOLOMON, R., 1992, A global biome model based on plant physiology and dominance, soil properties and climate. *Journal of Biogeography*, **19**, 117-134.
- PRINCE, S. D., 1991, A model of regional primary production for use with coarse resolution satellite data. *International Journal of Remote Sensing*, **12**, 1313-1330.
- QI, J., CHEHBOUNI, A., HUETE, A. R., KERR, Y. H., and SOROOSHIAN, S., 1994, A modified soil adjusted vegetation index. *Remote Sensing of Environment*, **48**, 119-126.
- ROBINSON, D. A., DEWEY, K. F., and HEIM, R. R., 1993, Global snow cover monitoring: An update. *Bulletin American Meteorological Society*, **74**, 1689-1696.
- RONDEAUX, G., and VANDERBILT, V. C., 1993, Specularly modified vegetation indices to estimate photosynthetic activity. *International Journal of Remote Sensing*, **15**, 1815-1823.
- RUNNING, S. W., 1990, Estimating terrestrial primary productivity by combining remote sensing and ecosystem simulation. In *Remote Sensing of Biosphere Functioning*, edited by R. Hobbs and H. Mooney (New York: Springer-Verlag), pp. 65-86.
- RUNNING, S. W., and HUNT JR, E. R., 1993, Generalization of a forest ecosystem process model for other biomes, BIOME-BGC, and an application for global-scale models. In *Scaling Physiological Processes: Leaf to Globe*, edited by J. R. Ehleringer and C. Field (London: Academic Press), pp. 141-158.
- RUNNING, S. W., NEMANI, R. R., PETERSON, D. L., BAND, L. E., POTTS, D. F., PIERCE, L. L., and SPANNER, M. A., 1989, Mapping regional forest evapotranspiration and photosynthesis by coupling satellite data with ecosystem simulation. *Ecology*, **70**, 1090-1101.
- RUNNING, S. W., LOVELAND, T. R., PIERCE, L. L., and HUNT, E. R. JR., 1994, A remote sensing based vegetation classification for global land cover analysis. *Remote Sensing of Environment* (in press).
- SELLERS, P. J., 1985, Canopy reflectance, photosynthesis and transpiration, *International Journal of Remote Sensing*, **6**, 1335-1372.
- SELLERS, P. J., HALL, F. G., ASRAR, G., STREBEL, D. E., and MURPHY, R. E., 1988, The first ISLSCP field experiment (FIFE). *Bulletin of American Meteorological Society*, **69**, 22-27.
- TANRÉ, D., VERMOTE, E., HOLBEN, B. N., and KAUFMAN, Y. J., 1992, Satellite Aerosol Retrieval over Land Surfaces using the Structure Functions. *IGARSS 1992 Proceedings*, pp. 1474-1477.
- TANS, P. P., FUNG, I. Y., and TAKAHASHI, T., 1990, Observational constraints on the global atmospheric CO₂ budget. *Science*, **247**, 1431-1438.
- TEILLET, P. M., and STAENZ, K., 1993, Atmospheric effects due to topography on MODIS vegetation index data simulated from AVIRIS imagery over mountainous terrain. *Canadian Journal of Remote Sensing*, **18**, 283-292.
- TOWNSHEND, J. R. G., JUSTICE, C., LI, W., GUERNEY, C., and MCMANUS, J., 1991, Global land cover classification by remote sensing: Present capabilities and future possibilities. *Remote Sensing of Environment*, **35**, 243-255.

- TOWNSHEND, J. R. G., JUSTICE, C., GURNEY, C., and MCMANUS, J., 1992, The impact of misregistration on change detection. *I.E.E.E. Transactions on Geoscience and Remote Sensing*, **30**, 1054-1060.
- TUCKER, C. J., TOWNSHEND, J. R. G., and GOFF, T. E., 1985, African land cover classification using satellite data. *Science*, **227**, 369-374.
- VERSTRAETE, M. M., PINTY, B., and DICKINSON, R. E., 1990, A physical model of the bidirectional reflectance of vegetation canopies: I. Theory. *Journal of Geophysical Research*, **95**, 11755-11765.
- WAN, Z., and DOZIER, J., 1989, Land-surface temperature measurement from space: physical principles and inverse modeling. *I.E.E.E. Transactions on Geoscience and Remote Sensing*, **27**, 268-278.